

# Accuracy of VIMOS night-time and daytime wavelength calibrations

---

Burkhard Wolff, Steffen Mieske, Juan Carlos Muñoz-Mateos, Sabine Möhler, Michael Hilker  
10 December 2014

## Abstract

Night-time calibrations that are attached to science OBs are mandatory for VIMOS MOS observations since early 2010 in order to be protected against instrumental flexures. The implementation of an Active Flexure Compensation (AFC) within the VIMOS upgrade project has reduced these flexures considerably. In this memo, we summarize investigations on the accuracy of MOS wavelength calibrations after the upgrade.

For the LR\_blue, LR\_red, and HR\_red grisms, we find accuracies of 0.5 to 1.0 pixel if calibrations are taken during daytime and not as attached night-time measurements. Science cases that do not require more accurate wavelength calibration can thus be executed without attached calibrations. For the three other grisms (MR, HR\_blue, and HR\_orange), we find uncertainties of 1.0 to 2.0 pixels when doing only daytime calibrations. We therefore strongly recommend to keep attached calibrations for these grisms.

## Data

Four different kinds of data sets have been used. The first one consists of randomly chosen pairs of night-time and daytime calibrations that were measured as part of regular operations with VIMOS. Examples for all grisms exist; data taken with four to seven different masks have been analyzed per grism.

The second set of data consists of series of flat-field and arc-lamp calibrations at different rotator angles. After each rotator movement, a full Active Flexure Compensation (AFC) has been applied. Calibrations for the LR\_blue grism (taken during the night of 2014-04-02) and for the MR grism (night of 2014-03-09) are included here.

The third data set has also sequences in rotator angle but an AFC was only applied in the beginning and not after every rotator movement. The HR\_red grism was used (nights of 2014-08-18 and 2014-08-19). The rotator angle was changed from +26.6 degrees to +116.0 degrees in steps of 10 degrees and back, and from +26.6 degrees to -63.4 degrees and back.

The fourth data set contains measurements with the same mask (and same grism) that were repeated on several days in September and October 2013. The goal was to investigate the influence of the mask exchange process.

## Analysis method

All calibrations have been processed using the vmmoscalib recipe of the VIMOS pipeline versions 2.9.7 (2014-03-09 data) and 2.9.13 (all other). For comparing different wavelength solutions, the MOS\_WAVELENGTH\_MAP pipeline products have been chosen. These files contain per detector pixel the wavelength (in Ångström) as derived from the wavelength solution of the pipeline and give, therefore, an easily accessible overview of the wavelength solution.

The wavelength maps from two different measurements are subtracted and give the difference map. The MOS\_SPATIAL\_MAP products are used to identify the areas of the slits on the detector. Furthermore, clipping has been applied to avoid strongly deviating pixels at the borders of the slits ( $\pm 20\text{Å}$  for LR and  $\pm 10\text{Å}$  for all other grisms). Then, the median of the difference map and the standard deviation are calculated and are divided by the nominal dispersion (in Å/pix) of each grism.

## Results: night-time vs. daytime calibrations

The results from comparing night-time wavelength calibrations against daytime calibrations are shown as one plot for each grism with one sub plot for each quadrant. The y axis has the median deviation in pixels; the error bars give the standard deviation. Values are plotted against the mask ID. The dotted horizontal lines are at  $\pm 1$  pixel deviation and can be taken as a reference for judging the quality. A global shift of the night-time wavelength calibration with respect to the daytime calibration results in a data point above or below zero in the plots. Large error bars indicate differences of the wavelength calibration for different parts of the spectrum. It has been verified for some examples that calculated deviations correspond to actual shifts in the positions of the arc lines in the raw data.

In the ideal case, the median deviation would be close to zero and would have a small standard deviation, i.e. well within the dispersion ( $\pm 1$  pixel). This is fulfilled only in few cases: mainly for most HR\_red and for some LR\_red data. All other grisms show rather large deviations for several night-day pairs and/or standard deviations of the order of or larger than 1 pixel.

Comments on individual data sets:

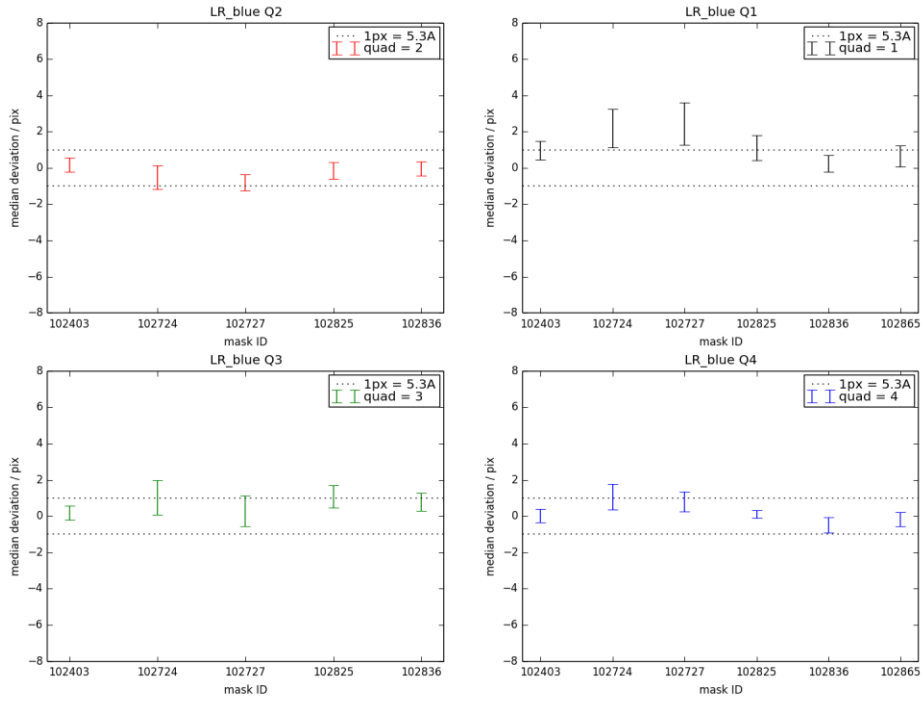
- LR\_blue: error bars are comparable to or smaller than the dispersion in many cases but there are also some strong deviations, especially in quadrant 1
- LR\_red: in general good, but also some deviating cases
- MR: error bars are comparable to the dispersion
- HR\_blue: pipeline results for the wavelength solution are in general not good; the calculated standard deviation may not be very meaningful
- HR\_orange: for quadrant 1, spectral lines are systematically shifted in different directions at the blue and red end; this explains the higher standard deviation
- HR\_red: in general good; poor wavelength solution by the pipeline for mask 2696 and quadrant 4 explains the higher standard deviation.

The table summarizes these results. All offsets are expressed in pixels so that values from different grisms can directly be compared. For each grism/quadrant combination, the offsets obtained with each mask measurement and the standard deviation of the difference maps have been averaged over all measurements (“mean offset” and “mean RMS”, respectively, in the table). A third data set in the table gives the standard deviation of the shifts obtained with different masks (“mask-to-mask scatter”). Average values per grism and per quadrant are added for all results.

The largest mean offsets appear for quadrant 1 but with significant differences between the grisms. LR\_red, MR, and HR\_red grisms show in general the smallest offsets, LR\_blue and HR\_blue the worst. With respect to the standard deviation of the shifts, HR\_blue and HR\_orange show very large changes for different parts of the masks. There is otherwise no overall dependency on the quadrant. There can, however, be significant differences from one measurement to the other, in particular for quadrants 1 and 4 and for the MR and HR\_orange grisms.

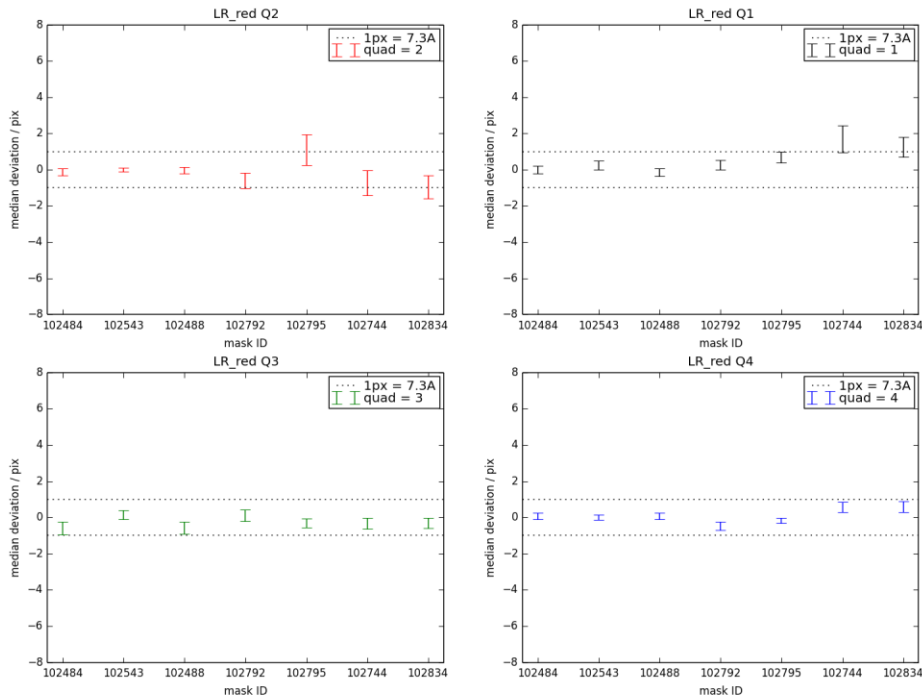
### Night-time vs. daytime wavelength calibrations

LR\_blue: WAVELENGTH\_MAP(night) - WAVELENGTH\_MAP(day)



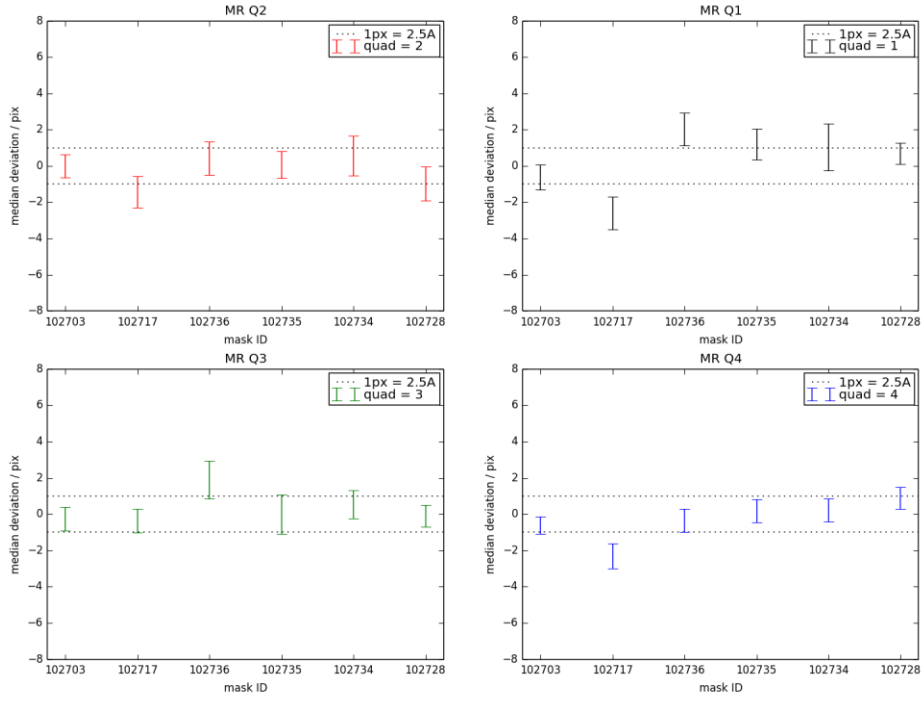
### Night-time vs. daytime wavelength calibrations

LR\_red: WAVELENGTH\_MAP(night) - WAVELENGTH\_MAP(day)



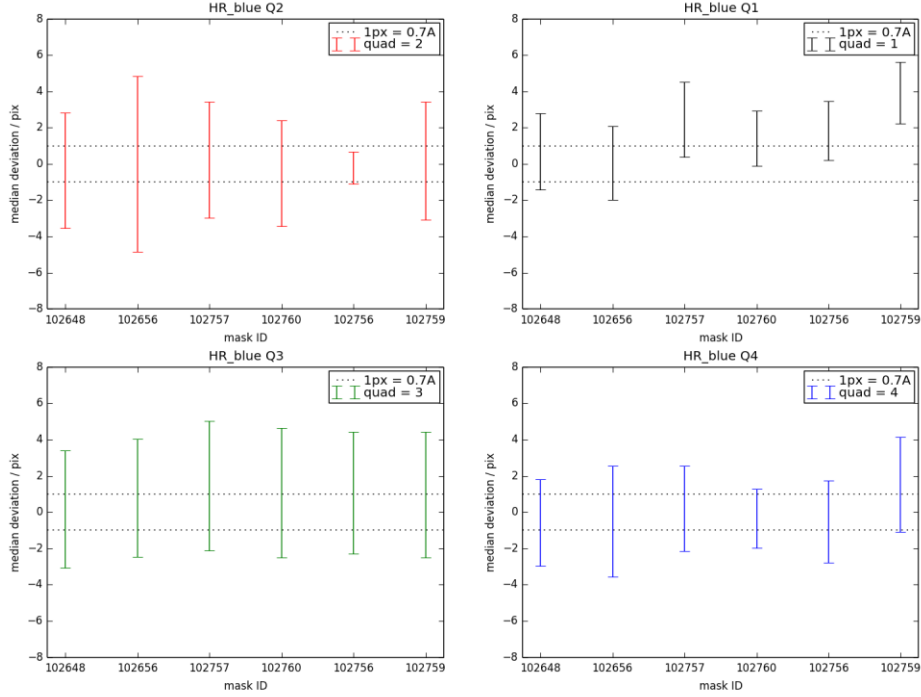
### Night-time vs. daytime wavelength calibrations

MR: WAVELENGTH\_MAP(night) - WAVELENGTH\_MAP(day)



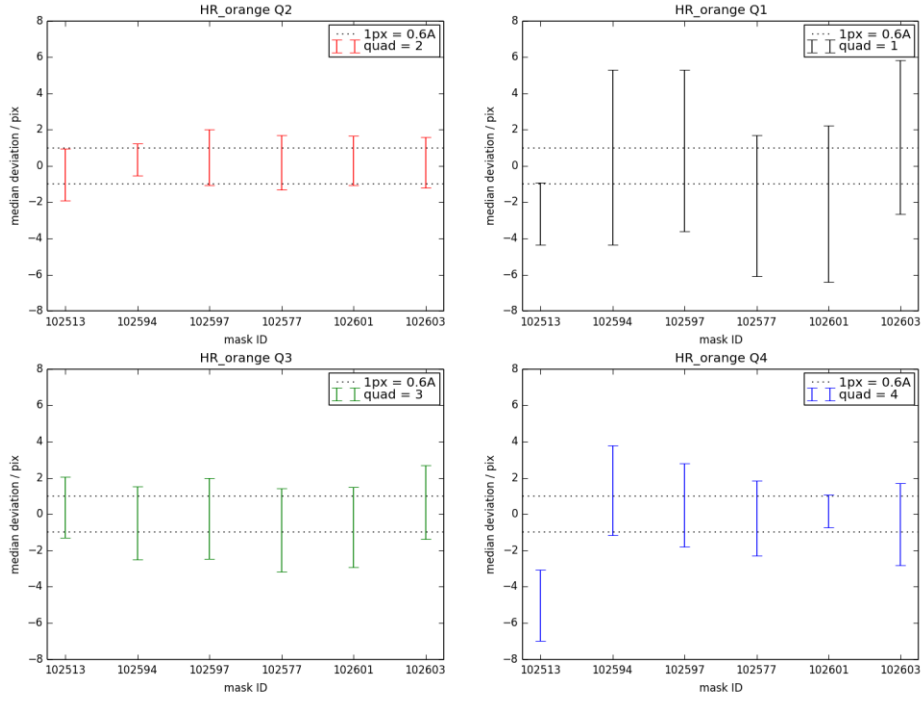
### Night-time vs. daytime wavelength calibrations

HR\_blue: WAVELENGTH\_MAP(night) - WAVELENGTH\_MAP(day)



### Night-time vs. daytime wavelength calibrations

HR\_orange: WAVELENGTH\_MAP(night) - WAVELENGTH\_MAP(day)



### Night-time vs. daytime wavelength calibrations

HR\_red: WAVELENGTH\_MAP(night) - WAVELENGTH\_MAP(day)

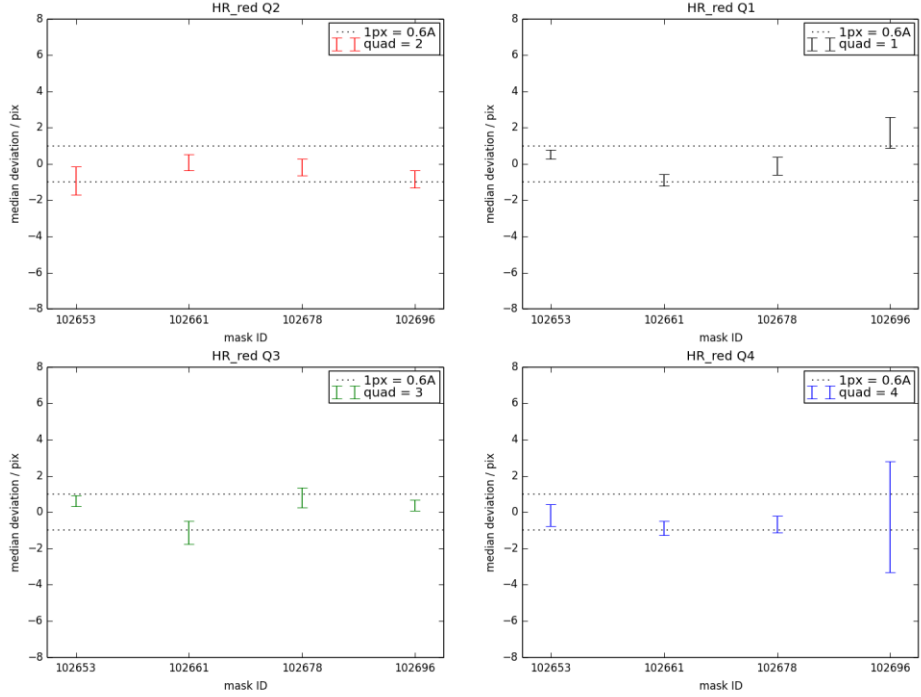


**Table: summary of night-time vs. daytime calibrations, expressed in pixel offsets**

	LR_blue	LR_red	MR	HR_blue	HR_orange	HR_red	Quadrant averages	Standard Deviation around average
mean offset Q1	1.265	0.567	0.28	1.71	-0.67	-0.16	<b>0.50</b>	0.81
mean offset Q2	-0.272	-0.195	-0.22	-0.12	0.17	-0.33	<b>-0.16</b>	0.16
mean offset Q3	0.675	-0.263	0.29	0.92	-0.21	0.19	<b>0.27</b>	0.43
mean offset Q4	0.2233	0.099	-0.33	-0.04	-0.64	-0.57	<b>-0.21</b>	0.33
<b>AVG</b>	<b>0.608825</b>	<b>0.281</b>	<b>0.28</b>	<b>0.6975</b>	<b>0.4225</b>	<b>0.3125</b>		
mean RMS Q1	0.74	0.36	0.87	1.84	3.9	0.35	<b>1.34</b>	1.25
mean RMS Q2	0.47	0.44	0.87	3.04	1.35	0.56	<b>1.12</b>	0.91
mean RMS Q3	0.66	0.3	0.8	3.4	2.07	0.5	<b>1.29</b>	1.10
mean RMS Q4	0.443	0.21	0.61	2.38	1.99	0.48	<b>1.02</b>	0.84
<b>AVG</b>	<b>0.57825</b>	<b>0.3275</b>	<b>0.7875</b>	<b>2.665</b>	<b>2.3275</b>	<b>0.4725</b>		
mask-to-mask scatter Q1	0.865	0.68	1.65	1.37	1.84	0.71	<b>1.19</b>	0.46
mask-to-mask scatter Q2	0.391	0.68	0.8	0.3	0.34	0.53	<b>0.51</b>	0.18
mask-to-mask scatter Q3	0.415	0.3	0.85	0.43	0.62	1.06	<b>0.61</b>	0.27
mask-to-mask scatter Q4	0.597	0.38	1.1	0.81	2.24	0.36	<b>0.91</b>	0.65
<b>AVG</b>	<b>0.567</b>	<b>0.51</b>	<b>1.1</b>	<b>0.7275</b>	<b>1.26</b>	<b>0.665</b>		

All results are normalized to the dispersion (in Å/pix), i.e. values are in pixels. Nominal dispersions are:

LR\_blue = 5.3 Å/pix; LR\_red = 7.3 Å/pix; MR = 2.5 Å/pix; HR\_blue = 0.71 Å/pix; HR\_orange = 0.6 Å/pix;

HR\_red = 0.6 Å/pix.

Mean offset: average over all measurements of each grism/quadrant combination of the mean deviation

Mean RMS: average over all measurements of each grism/quadrant combination of the standard deviation

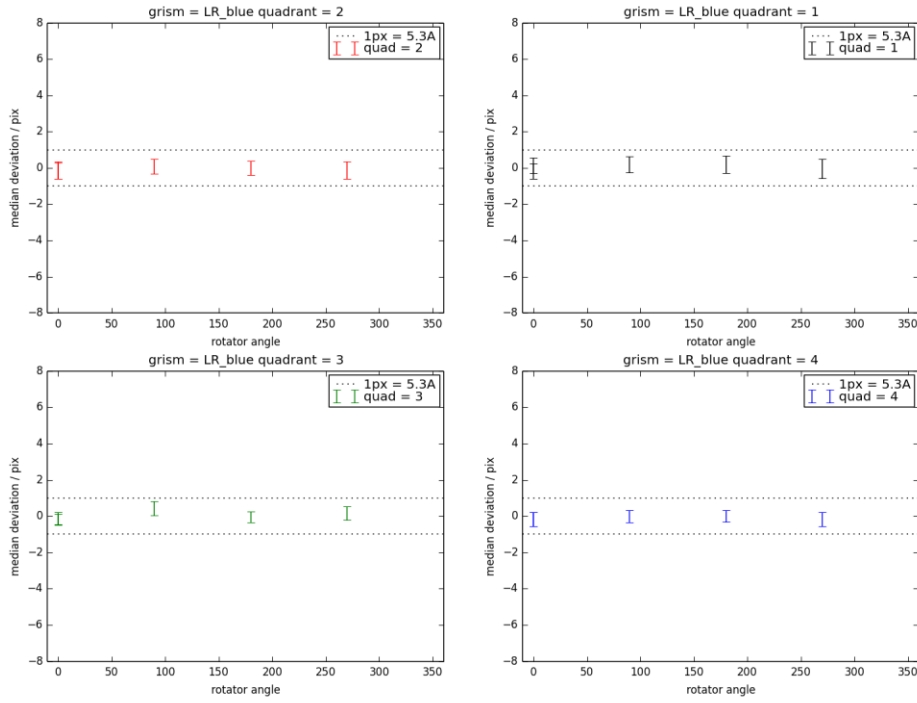
Mask-to-mask scatter: standard deviation of the mean deviation over all measurements per grism/quadrant combination

## **Results: rotator angle sequence with full AFC**

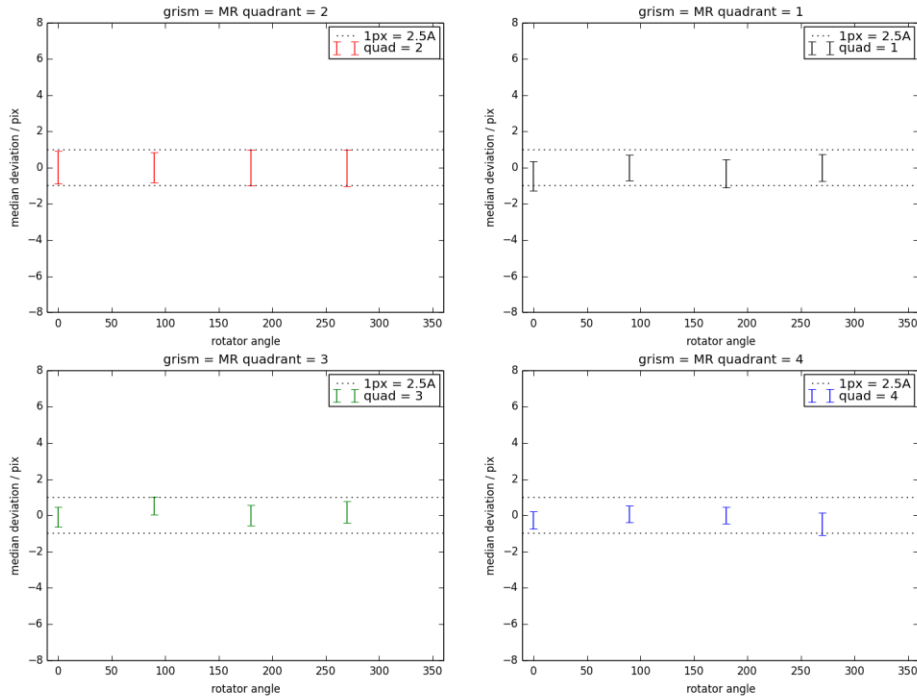
For analyzing the two calibration sequences with varying rotator angles, the map for 26.6 degrees, which is the normal rotator position for daytime calibrations, has been subtracted from the wavelength maps of the individual rotator positions. The plots are similar to the previous plots; the x axis now indicates the rotator angle.

In both data sets, taken with the LR\_blue and MR grisms, the standard deviations of the difference maps are much smaller than in the comparison of night-time with daytime calibrations. The median deviations are also much closer to zero. There does not seem to be a trend with respect to rotator angle. This indicates that the AFC does actually correct very well for instrumental flexures.

Rotator angle sequence: deviation of wavelength maps relative to 26.6  
2014-04-02, full AFC, LR\_blue



Rotator angle sequence: deviation of wavelength maps relative to 26.6  
2014-03-09, full AFC, MR+GG475

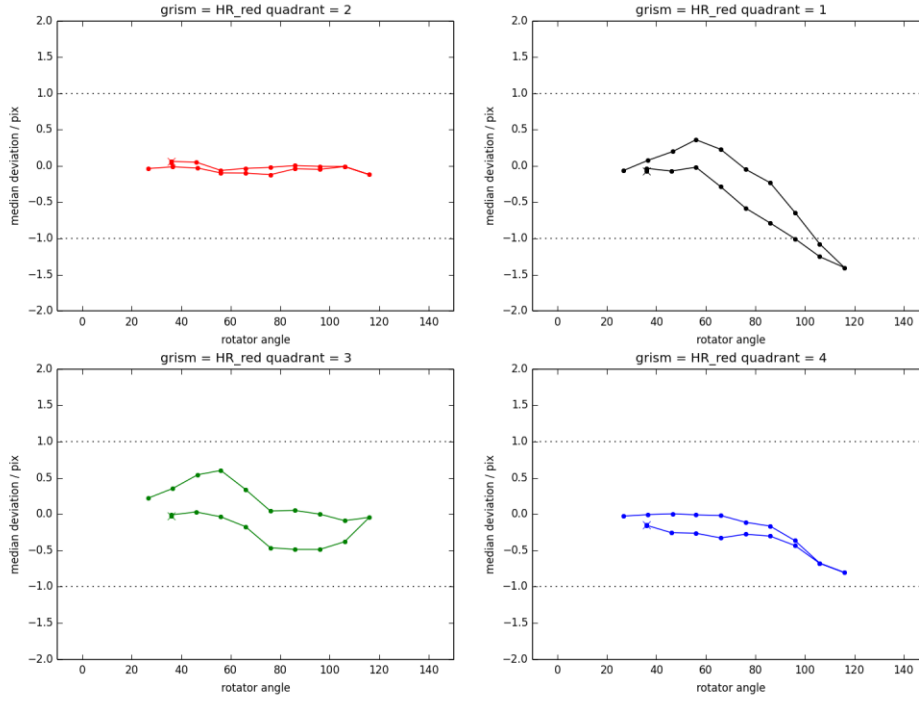


## **Results: rotator angle sequence without AFC**

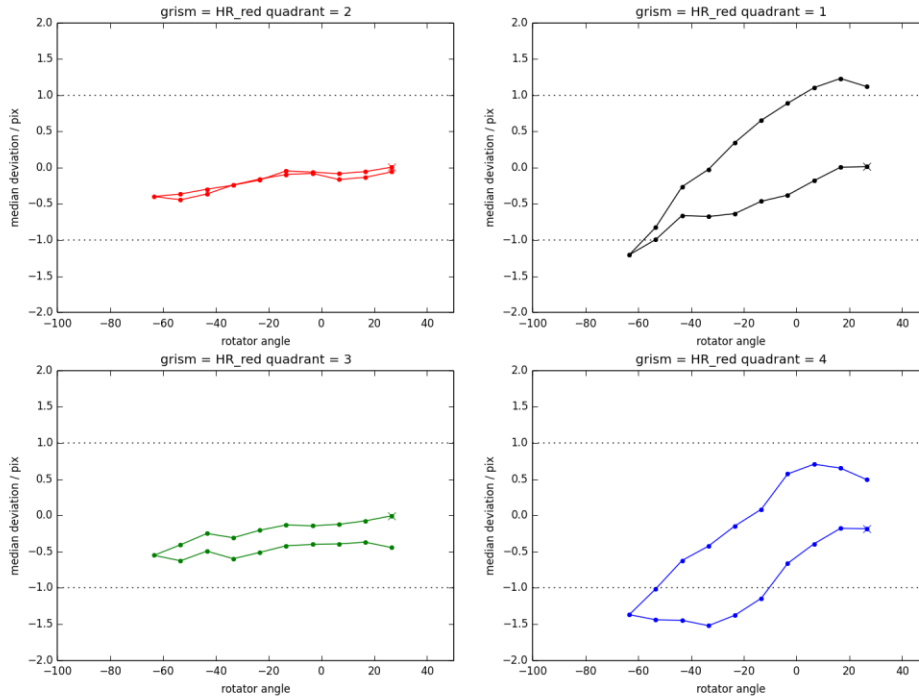
For analyzing the two rotator angle sequences without AFC, the first map at 26.6 degrees has been subtracted from the following maps. The second measurement is marked with a cross in the plots. (In the sequence going from 26.6 to -63.4 degrees, the calibration at 26.6 degrees has been repeated in the beginning). Standard deviations of the difference maps have not been plotted here in order to see the movement of the median deviation more clearly. They are smaller than 1 pixel.

Quadrant 1 shows significant offsets from the original position in both sequences, quadrant 4 only in the sequence from 26.6 to -63.4 degrees. In this sequence, a hysteresis is visible after returning to the original rotator angle whereas the offsets vanish in the other sequence at the end. Deviations in quadrants 2 and 3 are only minimal.

Rotator angle sequence: deviation of wavelength maps relative to start at 26.6  
26.6 to +116.0 and back

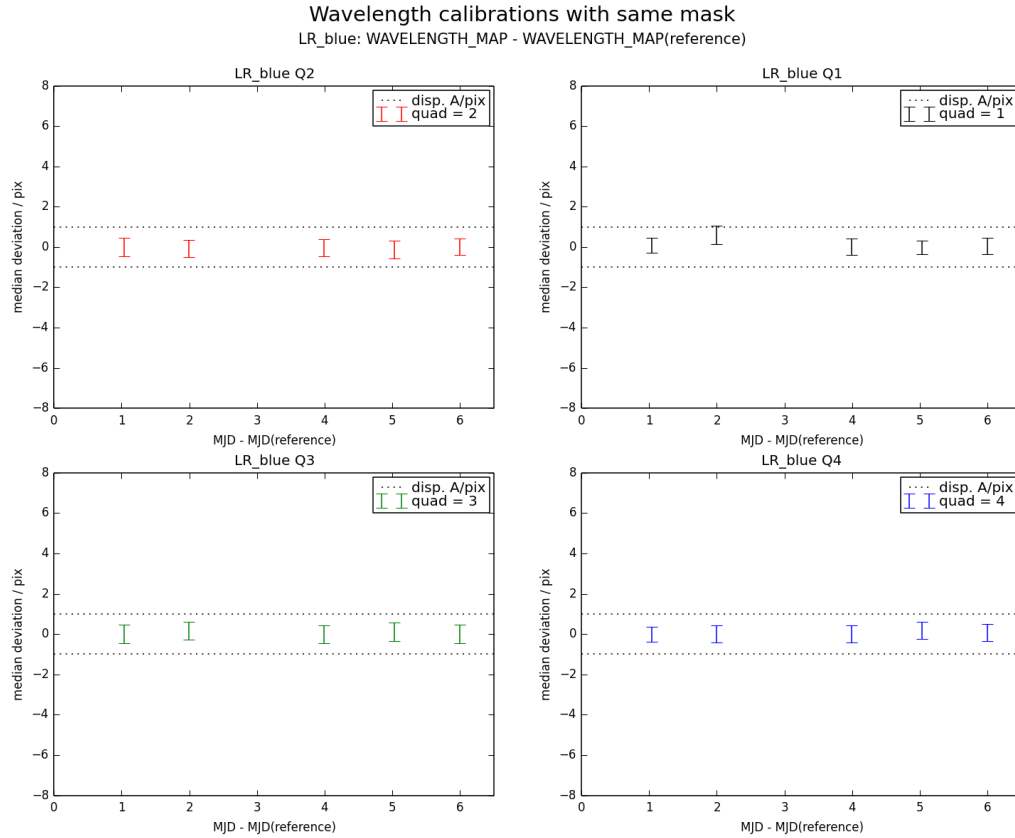


Rotator angle sequence: deviation of wavelength maps relative to start at 26.6  
26.6 to -63.4 and back



## Results: calibrations with same mask

Several daytime calibrations with mask 2744 and the LR\_blue grism, taken in September and October 2013 on different days, were analyzed. They show a quality comparable to the measurements using full AFC over a rotator angle sequence. This basically rules out that the mask exchange is the cause for the large offsets that have been found in the comparison of daytime with attached night-time calibrations.



## Conclusions

The results of our tests are summarized in the table where we give the offsets between night-time and daytime wavelength calibrations in pixels, as a function of grism and quadrant, averaged over the various mask sets investigated. Median deviations in the difference maps can be as large as two pixels for some grisms, in particular in quadrant 1. The standard deviations of these maps are between 0.5 and 1 pixel for most grisms, but much worse (2-3 pixels) for the HR\_blue and HR\_orange grisms. In general, we thus recommend to use attached night-time calibrations for scientific cases that require wavelength calibration accuracies of better than 1 pixel. For other applications it may be sufficient to use daytime calibrations only, especially in the more accurate cases of the LR\_red and HR\_red grisms, which give wavelength calibration reproducibility down to about 0.5 pixels between night-time and daytime calibrations. Users are advised to refer to the table for achievable accuracies of daytime calibrations.

Note that the two rotator angle sequences do show a good reproducibility well below the 1 pixel limit. We attribute this to the fact that an AFC was executed before each calibration measurement here whereas during night-time observations the AFC is applied only before the acquisition: the instrument rotates freely between AFC correction and the night-time calibration which introduces some flexure compared to the fully AFC-corrected position in the daytime calibrations. This rotation can amount to several tens of degrees.

The effect is investigated in the following figure where the average offset per mask is plotted against the difference of the rotator angle between AFC and attached calibrations (for measurements with LR\_blue, LR\_red, MR, and HR\_red grisms). There is a weak indication for a correlation between offsets and rotator angle difference in quadrant 1, consistent with the overall larger deviations found for this quadrant. On the other hand, the mask exchange between night and day does not seem to play a role.

The results of this investigation show that it is in general necessary to use attached night-time arc-lamp exposures for calibrating MOS science observations if one requires wavelength calibration accuracy better than about 1 pixel. The underlying reason for this is that the corrections of the current VIMOS Active Flexure Compensation are partially altered again by instrument rotations that are necessary to either follow the object on sky or to change optical elements. The VIMOS IOT is investigating possibilities to optimize the AFC procedures of VIMOS.

